

1 **Some insights into the condensing vapors driving new particle**  
2 **growth to CCN sizes on the basis of hygroscopicity measurements**

3 **Z. J. Wu<sup>1,2</sup>, L. Poulain<sup>2</sup>, W. Birmili<sup>2</sup>, J. Größ<sup>2</sup>, N. Niedermeier<sup>2</sup>, Z. B. Wang<sup>3</sup>, H.**  
4 **Herrmann<sup>2</sup>, A. Wiedensohler<sup>2</sup>**

5 [1] College of Environmental Sciences and Engineering, Peking University, 100871, Beijing, China

6 [2] Leibniz Institute for Tropospheric Research, 04318, Leipzig, Germany

7 [3] Multiphase Chemistry Department, Max Planck Institute for Chemistry, Mainz 55128, Germany

8 Correspondence to: Zhijun Wu ([zhijunwu@pku.edu.cn](mailto:zhijunwu@pku.edu.cn))

9 **Abstract**

10 New particle formation (NPF) and growth is an important source of cloud condensation nuclei  
11 (CCN). In this study, we investigated the chemical species driving new particle growth to the  
12 CCN sizes on the basis of particle hygroscopicity measurements carried out at the research  
13 station Melpitz, Germany. Three consecutive NPF events occurred during summertime were  
14 chosen as examples to perform the study. Hygroscopicity measurements showed that the  
15  $(\text{NH}_4)_2\text{SO}_4$ -equivalent water-soluble fraction respectively accounts for 20% and 16% of 50 and  
16 75 nm particles during the NPF events. Numerical analysis showed the ratios of  $\text{H}_2\text{SO}_4$   
17 condensational growth to the observed particle growth were 20% and 13% for 50 and 75 nm  
18 newly formed particles, respectively. Aerosol mass spectrometer measurements showed that an  
19 enhanced mass fraction of sulfate and ammonium in the newly formed particles was observed  
20 when new particle grew to the sizes larger than 30 nm shortly after the particle formation period.  
21 At a later time, the secondary organic species played a key role in the particle growth. Both  
22 hygroscopicity and AMS measurements and numerical analysis confirmed that organic  
23 compounds were major contributors driving particle growth to CCN sizes. The critical diameters  
24 at different supersaturations estimated using AMS data and  $\kappa$ -Köhler theory increased  
25 significantly during the later course of NPF events. This indicated that the enhanced organic  
26 mass fraction caused a reduction in CCN efficiency of newly formed particles. Our results  
27 implied that the CCN production associated with atmospheric nucleation may be overestimated if  
28 assuming that newly formed particles can serve as CCN in case they grow to a fixed particle size,  
29 which was used in some previous studies, especially for organic-rich environments. In our study,

1 the enhancement in CCN number concentration associated with individual NPF events have been  
2 63%, 66%, and 69% for supersaturation 0.1%, 0.4%, and 0.6%, respectively.

### 3 **1 Introduction**

4 The formation of new particles from gaseous precursors and their subsequent growth represent a  
5 key stage in the lifecycle of atmospheric aerosol particles. This new particle formation (NPF)  
6 process represents an important source of atmospheric particles and possibly also for the number  
7 concentration of cloud condensation nuclei (CCN) (Spracklen et al., 2008;Wiedensohler et al.,  
8 2009;Wang and Penner, 2009;Laaksonen et al., 2005;Yue et al., 2011;Kazil et al.,  
9 2010;Sotiropoulou et al., 2006;Laakso et al., 2013) . NPF has thus the potential to influence  
10 climatologically important processes such as precipitation patterns and Earth's energy balance  
11 (Paasonen et al., 2013). The contribution of atmospheric nucleation to the global CCN budget  
12 spans a relatively large uncertainty range, which, together with our general poor understanding  
13 of aerosol-cloud interactions, results in major uncertainties in the radiative forcing by  
14 atmospheric aerosols (Kerminen et al., 2012). Recent model studies (Spracklen et al.,  
15 2008;Merikanto et al., 2009;Westervelt et al., 2014) have attempted to elaborate on the  
16 connection between NPF and CCN production, a process that is sensitive to a number of  
17 environmental factors.

18 Freshly formed particles are about 1 nanometers in diameter (Kulmala et al., 2012), and they  
19 must grow tens of nanometers in order to serve as a CCN (Dusek et al., 2006;Kerminen et al.,  
20 2012). Apparently, the nucleation rate, the particle growth, and the rate by which growing  
21 particles are removed by coagulation or deposition greatly influence the CCN production  
22 associated with atmospheric nucleation (Kuang et al., 2009;Kerminen et al., 2004). From the  
23 point of view of chemical species, both sulfuric acid and organics contribute to the subsequent  
24 particle growth after nucleation (Smith et al., 2004;Pierce et al., 2011;Ehn et al., 2007;Kulmala et  
25 al., 2004;Brus et al., 2011;Kulmala et al., 2006;Sipilä et al., 2010;Zhang et al., 2004b;Kiendler-  
26 Scharr et al., 2009;Wang et al., 2010;Ristovski et al., 2010). The contribution of sulfate and  
27 organics in the particle growth seems to be strongly depending on the location (e.g. Yue et al.,  
28 2010;Boy et al., 2005). For example, sulfuric acid fully explains the particle growth observed in  
29 the polluted urban areas, Atlanta, USA (Stolzenburg et al., 2005), while it represents only 10% in  
30 Boreal forest area (Boy et al., 2005).

1 Due to the differences in hygroscopicity of sulfuric acid and/or its ammonium salts and  
2 secondary organic compounds (Virkkula et al., 1999;Varutbangkul et al., 2006;Tang and  
3 Munkelwitz, 1994), hygroscopicity measurements during a NPF event can provide insight into  
4 the changes in condensing vapor properties and chemical composition of newly formed particles  
5 (Hämeri et al., 2001;Ehn et al., 2007;Ristovski et al., 2010). In this study, we investigated the  
6 chemical species driving new particle growth into CCN sizes by using experimental data on  
7 particle hygroscopicity and chemical composition measured at Melpitz, Germany. In addition,  
8 the production of potential CCN associated with the NPF event was evaluated.

## 9 **2 Measurements**

10 Atmospheric measurements were performed at the research station Melpitz, Germany (51.54°N,  
11 12.93°E, 86 m above sea level). The atmospheric aerosol observed at Melpitz can be regarded as  
12 representative for Central European background conditions (Birmili et al., 2009). An account of  
13 the NPF process at Melpitz and its relationship with precursor gases and meteorology can be  
14 found in Größ et al. (2015).

15 The data of this study were collected during the European Integrated Project on Aerosol Cloud  
16 Climate Air Quality Interactions (EUCAARI, (Kulmala et al., 2009)) intensive field campaign  
17 from May 23<sup>rd</sup> to June 8<sup>th</sup> in 2008. Table 1 summarizes the instruments and measured parameters  
18 used in this study. All instruments were set up in the same container laboratory and utilized the  
19 same air inlet. The inlet line consisted of a PM<sub>10</sub> Anderson impactor located approximately 6 m  
20 above ground level and directly followed by an automatic aerosol diffusion dryer (Tuch et al.,  
21 2009) that maintained the relative humidity in the sampling line below 30%. Particle  
22 hygroscopicity, particle number size distribution, and chemical composition of non-refractory  
23 PM<sub>1</sub> were determined using a hygroscopicity tandem differential mobility particle analyzer (H-  
24 TDMA), a Twin Differential Mobility Particle Sizer (TDMPS), and a High Resolution Time-of-  
25 flight Aerosol Mass Spectrometer (HR-Tof-AMS), respectively.

### 26 **2.1 Particle hygroscopicity measurements**

27 The H-TDMA used in this study has been described in previous publications in detail (Wu et al.,  
28 2011;Massling et al., 2003), and complies to the instrumental standards prescribed in Massling et  
29 al. (2011). The H-TDMA consists of three main parts: (1) A Differential Mobility Analyzer  
30 (DMA1) that selects quasi-monodisperse particles at a relative humidity below 10%, and a

1 Condensation Particle Counter (CPC1) that measures the particle number concentration leaving  
 2 DMA1 at the selected particle size; (2) An aerosol humidifier conditioning the particles selected  
 3 by DMA1 to a defined relative humidity (RH); (3) The second DMA (DMA2) coupled with  
 4 another condensation particle counter (CPC2) to measure the number size distributions of the  
 5 humidified aerosol. DMA2 and the aerosol humidification are placed in a temperature-controlled  
 6 box. Hygroscopicity scans with 100 nm ammonium sulfate particles were performed frequently  
 7 to analyze the stability of the relative humidity of 90% in the second DMA. Hygroscopicity  
 8 measurements with RH between 87% and 90% were accepted for further analysis.

9 The hygroscopic growth factor (HGF) is defined as the ratio of the particle mobility diameter,  
 10  $D_p(\text{RH})$ , at a given RH to the dry diameter,  $D_{p,\text{dry}}$ :

$$11 \quad \text{HGF}(\text{RH}) = \frac{D_p(\text{RH})}{D_{p,\text{dry}}} \quad [1]$$

12 The TDMA<sub>inv</sub> method developed by Gysel et al. (2009) was used to invert the H-TDMA data.  
 13 Dry scans (RH<10%) were used to calibrate a possible offset between DMA1 and DMA2 and  
 14 define the width of the H-TDMA's transfer function (Gysel et al., 2009). In this study, the  
 15 particles with dry sizes of 35, 50, 75, 110, 165, and 265 nm were measured by H-TDMA at  
 16 RH=90% with the time resolution of 1h. The HGFs of 35, 50, and 75 nm particles will be taken  
 17 for further analysis.

18 The hygroscopicity parameter,  $\kappa$ , can be calculated from the HGF measured by H-TDMA  
 19 (Petters and Kreidenweis, 2007):

$$20 \quad \kappa_{\text{HTDMA}} = (\text{HGF}^3 - 1) \left( \frac{\exp\left(\frac{A}{D_{p,\text{dry}} \cdot \text{HGF}}\right)}{\text{RH}} - 1 \right) \quad [2]$$

$$21 \quad A = \frac{4\sigma_{s/a}M_w}{RT\rho_w} \quad [3]$$

22 Where  $D_{p,\text{dry}}$  and HGF are the initial dry particle diameter and the hygroscopic growth factor at  
 23 90% RH measured by H-TDMA, respectively.  $\sigma_{s/a}$  is the droplet surface tension (assumed to be  
 24 that of pure water,  $\sigma_{s/a} = 0.0728 \text{ N m}^{-2}$ ),  $M_w$  the molecular weight of water,  $\rho_w$  the density of  
 25 liquid water, R the universal gas constant, and T the absolute temperature.

## 1 **2.2 Particle chemical composition**

2 The Aerodyne HR-ToF-AMS (here simply referred to as AMS) (DeCarlo et al., 2006) was  
3 operated with a time resolution of 5 min. Due to the 600 °C surface temperature of the vaporizer,  
4 the AMS only analyzes the non-refractory chemical composition of the particles. Soot, crustal  
5 material, and sea-salt cannot be detected. The aerodynamic lenses have 100% transmission  
6 efficiency down to 70 nm in a vacuum aerodynamic diameter (Canagaratna et al., 2007).  
7 Therefore, based on the transmission efficiency of the aerodynamic lenses and the detected  
8 compounds, the AMS can provide the size-resolved chemical composition of sub-micrometer  
9 non-refractory aerosol particle fraction (NR-PM1) (Canagaratna et al., 2007). The vacuum  
10 aerodynamic diameter for AMS measurements was converted to mobility diameter by division of  
11 AMS vacuum aerodynamic diameter by the estimated particle density (1400 kg/m<sup>3</sup>). Hereafter,  
12 the mobility diameter is used in AMS data below. The particle density was calculated on the  
13 basis of measured chemical composition. The detail description can be found in Poulain et al.  
14 (2014).

## 15 **2.3 Particle number size distribution**

16 A TDMPS was deployed to measure particle number size distributions from 3-800 nm mobility  
17 diameter with a time resolution of 10 min (Birmili et al., 1999). The system consists of two  
18 Differential Mobility Analyzers (DMA, Hauke-type) and two Condensation Particle Counters  
19 (CPC, TSI model 3010 and TSI model 3025). The sheath air is circulated in closed loops for both  
20 DMAs. Evaluation of particle number size distributions includes a multiple charge inversion, the  
21 CPC efficiency and diffusional losses in the DMA and all internal and external sampling lines  
22 according to the recommendations in Wiedensohler et al. (2012).

## 23 **3 Methodology**

### 24 **3.1 Derivation of the soluble particle fraction**

25 Based on the Zdanovskii–Stokes–Robinson (ZSR) method (Stokes and Robinson,  
26 1966; Zdanovskii, 1948), the HGF of a mixture can be estimated from the sum of HGF<sub>*i*</sub> of a pure  
27 component (*i*) time their respective volume fractions, ε<sub>*i*</sub> (Malm and Kreidenweis, 1997):

$$28 \text{HGF}_{\text{mixed}} = (\sum_i \varepsilon_i \text{HGF}_i^3)^{1/3} \quad [4]$$

1 Here, the chemical compounds contributing to the particle growth are separated into two fractions,  
2 i.e., soluble and insoluble fractions (also refer to Ehn et al., 2007; Swietlicki et al., 1999). The  
3 soluble fraction is assumed as ammonium sulfate and the insoluble fraction as organic  
4 compounds. Then,  $\epsilon$  of soluble fraction can be calculated by:

$$5 \quad \epsilon_{\text{soluble}} = \frac{\text{HGF}_{\text{measured}}^3 - 1}{\text{HGF}_{(\text{NH}_4)_2\text{SO}_4}^3 - 1} \quad [5]$$

6 where  $\text{HGF}_{\text{measured}}$  is the HGF of particle measured by H-TDMA, and  $\text{HGF}_{(\text{NH}_4)_2\text{SO}_4}$  is the HGF  
7 of pure  $(\text{NH}_4)_2\text{SO}_4$  particle with the same size. When calculating  $\text{HGF}_{(\text{NH}_4)_2\text{SO}_4}$  in different  
8 diameters, the parameterizations for  $(\text{NH}_4)_2\text{SO}_4$  water activity developed by Potukuchi and  
9 Wexler (1995) and the density reported by Tang and Munkelwitz (1994) are used. The Kelvin  
10 term was considered in the calculation.

11 The assumption of an insoluble organic fraction may lead to overestimate of the soluble fraction  
12 because atmospherically relevant secondary organics typically have a growth factor larger than 1  
13 (e.g., Varutbangkul et al., 2006). This implies that in the presence of several classes of  
14 hygroscopic substances,  $\epsilon$  derived from Eq. [5] is only an “equivalent” soluble fraction (i.e.  
15 assuming ammonium sulfate as the only soluble substance).  $\epsilon_{\text{soluble}}$  is therefore an upper estimate  
16 for the true soluble volume fraction. The advantage of using the equivalent water-soluble fraction  
17 term is to be able to analyze the particle hygroscopicity independently of differences in size. The  
18 uncertainty of the estimated soluble volume fraction is around 5%, which was derived from the  
19 measurement uncertainty of HGF (2.5%) according to the error propagation function.

### 20 **3.2 Calculation of CCN number concentration**

21 The CCN number concentration can be estimated by integrating the particle number size  
22 distribution from the critical diameter to the maximum diameter detected by TDMPS (800 nm,  
23 above which the particle number concentration is generally negligible), assuming particles are  
24 internal mixture. The critical diameter ( $D_{\text{pcrit}}$ ) is calculated from  $\kappa$ :

$$25 \quad D_{\text{Pcrit}} = \left( \frac{4A^3}{27\kappa_{\text{chem}} \ln^2 S_c} \right)^{1/3} \quad [6]$$

26 Here,  $D_{\text{Pcrit}}$  is the critical diameter at which 50% of the particles were activated at the  
27 supersaturation,  $S_c$  (0.1%, 0.4%, and 0.6% were chosen in this study).  $\kappa_{\text{chem}}$  is calculated from

1 size-resolved AMS data according to the ZSR method and  $\kappa$ -Köhler theory (Petters and  
2 Kreidenweis, 2007):

$$3 \quad \kappa_{\text{chem}} = \sum_i \varepsilon_i \kappa_i \quad [7]$$

4 Here,  $\kappa_i$  and  $\varepsilon_i$  are the hygroscopicity parameter and volume fraction for the individual (dry)  
5 component in the mixture with  $i$ , the number of components in the mixture. The volume fraction  
6 of each chemical species in the mixture was derived from the size-resolved AMS data as  
7 described below.

8 Particle mass size distributions of organics, sulfate ( $\text{SO}_4^{2-}$ ), nitrate ( $\text{NO}_3^-$ ), and ammonium ( $\text{NH}_4^+$ )  
9 ions were detected by AMS. We use a simplified ion pairing scheme as presented in Gysel et al.  
10 (2007) to convert the ion mass concentrations to the mass concentrations of their corresponding  
11 inorganic salts as listed in Table 2. The critical diameters, corresponding to supersaturation (SS)  
12 0.2-0.6%, roughly spanned from 50 to 120 nm in mobility diameter. Therefore, by integrating the  
13 particle mass size distribution from 50 nm to 120 nm, the mass concentrations of organics,  $\text{SO}_4^{2-}$ ,  
14  $\text{NO}_3^-$ , and  $\text{NH}_4^+$  ions was calculated to estimate  $\kappa_{\text{chem}}$ . In the same way, the chemical  
15 composition of 150-200 nm particles is used to calculate  $\kappa_{\text{chem}}$  for the critical diameter of around  
16 170 nm, which corresponds to a supersaturation of 0.1%.

17 The H-TDMA-derived  $\kappa$  was not used in calculating the critical diameter. This reason is given as  
18 follows: The inconsistencies between H-TDMA-derived kappa and Cloud Condensation Nuclei  
19 Counter (CCNc)-derived  $\kappa$  have been reported in several previous studies (Good et al.,  
20 2010; Cerully et al., 2011; Irwin et al., 2010; Petters et al., 2009; Wex et al., 2009). Possible  
21 explanations are non-ideality effects in the solution droplet, surface tension reduction due to  
22 surface active substances, and the presence of slightly soluble substances which dissolve at RHs  
23 larger than the one considered in the H-TDMA (Wex et al., 2009). Due to these effects,  $\kappa$  is not  
24 necessarily constant and may vary with humidity. Extrapolating from H-TDMA data to  
25 properties at the point of activation should be done with great care (Wu et al., 2013). In addition,  
26 our previous study (Wu et al., 2013) showed that critical diameters at different supersaturations  
27 can be well-predicted using AMS data and ZSR method. Therefore, the AMS data was decided  
28 to use to estimate the critical diameters instead of H-TDMA-derived  $\kappa$ .

### 1 3.3 Estimation of H<sub>2</sub>SO<sub>4</sub> concentration

2 H<sub>2</sub>SO<sub>4</sub> concentrations were estimated using a modified version of the chemical mass balance  
3 model introduced by Weber et al. (1997), driven by solar radiation as a source of OH:

$$4 \quad [\text{H}_2\text{SO}_4] = B \frac{[\cdot\text{OH}][\text{SO}_2]}{\text{CS}} \quad [\text{cm}^{-3}] \quad [8]$$

5 Here, [ $\cdot\text{OH}$ ] is the hydroxyl radical concentration estimated from Eq. [9] in  $\text{cm}^{-3}$ . [ $\text{SO}_2$ ] is the  
6 measured sulfur dioxide concentration in  $\text{cm}^{-3}$ .  $B$  is a constant related to the reaction rate of the  
7 two species. CS is the condensation sink (Pirjola et al., 1999) in  $\text{s}^{-1}$  calculated from the particle  
8 number size distribution adjusted to ambient relative humidity. For this adjustment, an empirical  
9 growth law based on one year of hygroscopicity measurements at Melpitz was used (Refer to  
10 Laakso et al., 2004). The term  $B[\cdot\text{OH}][\text{SO}_2]$  represents the production term of H<sub>2</sub>SO<sub>4</sub>, and CS  
11 refers to represent the loss rate of H<sub>2</sub>SO<sub>4</sub> on the pre-existing particles.  $B$  was derived by  
12 correlation analysis of measured and estimated [ $\text{H}_2\text{SO}_4$ ] for 9 days during EUCAARI-2008  
13 during which the data capture was satisfactory. Linear regression analysis yielded a value of  
14  $27.49 \cdot 10^{-13} \text{ cm}^3 \text{ s}^{-1}$  for  $B$ .

$$15 \quad [\cdot\text{OH}] = A' \cdot \text{Rad} \quad [\text{cm}^{-3}] \quad [9]$$

16 where Rad is the global solar radiation flux in  $\text{W m}^{-2}$ .  $A'$  was derived by linear regression of  
17 these parameters for the EUCAARI-2008 data set, yielding a value of  $6166 \text{ m}^2 \text{ W}^{-1}$  for  $A'$ . The  
18 calculation of H<sub>2</sub>SO<sub>4</sub> concentration was done within the works of Größ et al. (2015), with details  
19 provided therein. The accuracy of simulated H<sub>2</sub>SO<sub>4</sub> concentration is estimated as follow:  
20 Percentage error =  $\text{abs}([\text{H}_2\text{SO}_4]_{\text{measured}} - [\text{H}_2\text{SO}_4]_{\text{simulated}}) * 100 / [\text{H}_2\text{SO}_4]_{\text{simulated}}$ . Here,  
21  $[\text{H}_2\text{SO}_4]_{\text{measured}}$  is the sulfuric acid concentration measured during 9-day measurements for  
22 EUCAARI-2008. The percentage error is around 40%.

### 23 3.4 Calculation of particle formation and growth rate

24 Assuming a constant particle source during a time period of  $t$ , the particle formation rate ( $J_{\text{nuc}}$ )  
25 can be expressed as (Dal Maso et al., 2005):

$$26 \quad J_{\text{nuc}} = \frac{dN_{\text{nuc}}}{dt} + F_{\text{coag}} + F_{\text{growth}} \quad [10]$$

27 In this study,  $N_{\text{nuc}}$  is the number concentration of nucleation mode particles ranging from 3 nm to  
28 25 nm.  $F_{\text{growth}}$  is the flux of particles out of the specified size range (3-25 nm). The newly formed



1 particles rarely grew beyond 25 nm before formation ended, and  $F_{\text{growth}}$  can be neglected.  $F_{\text{coag}}$   
 2 represents a loss of formed particles due to coagulation to the preexisting particle population. It  
 3 can be calculated from the following equation:

$$4 \quad F_{\text{coag}} = \text{Coag}S_{\text{nuc}}N_{\text{nuc}} \quad [11]$$

5 where  $\text{Coag}S_{\text{nuc}}$  is the coagulation sink of particles in the nucleation mode. The detailed  
 6 calculation of coagulation sink is given in Deal Maso et al. (2005).

7 The observed particle growth rate ( $\text{GR}_{\text{obs}}$ ) can be expressed as:

$$8 \quad \text{GR}_{\text{obs}} = \frac{\Delta D_m}{\Delta t} \quad [12]$$

9 where  $D_m$  is a geometric mean diameter of log-normal ultrafine particle mode, which has been  
 10 fitted to the number size distribution (Heintzenberg, 1994).  $\text{GR}_{\text{obs}}$  means evolution of the mean  
 11 diameter within a time period  $\Delta t$ .

### 12 **3.5 Particle growth contributed by H<sub>2</sub>SO<sub>4</sub> condensation**

13 Theoretically, the vapor concentration required for growth rate of 1 nm h<sup>-1</sup> in certain particle size  
 14 ranges can be calculated according to (Nieminen et al., 2010):

$$15 \quad C_{\text{GR}=1\text{nm}/\text{h}} = \frac{2\rho_v d_v}{\gamma m_v \Delta t} \cdot \sqrt{\frac{\pi m_v}{8kT}} \cdot \left[ \frac{2x_1+1}{x_1(x_1+1)} - \frac{2x_0+1}{x_0(x_0+1)} + 2\ln\left(\frac{x_1(x_0+1)}{x_0(x_1+1)}\right) \right] \quad [13]$$

16 here  $x_0$  and  $x_1$  are the ratios of the vapour molecule diameter ( $d_v$ ) to the initial and final particle  
 17 diameter, respectively. The mass ( $m_v$ ) and density ( $\rho_v$ ) of sulfuric acid applied in this study are  
 18 135 amu and 1650 kg/m<sup>3</sup>, respectively, corresponding to hydrated sulfuric acid molecules  
 19 (Kurtén et al., 2007). It should be mentioned that equation [13] was developed specially for  
 20 particles with diameter of 3-7 nm. For larger particles (>10 nm), this method gives similar results  
 21 to that calculated using the Fuchs-Sutugin approach (Nieminen et al., 2010). The calculated  
 22  $C_{\text{GR}=1\text{nm}/\text{h}, \text{H}_2\text{SO}_4}$  may be an underestimate because it is assumed that every sulfuric acid molecule  
 23 colliding with the particle is attached to it which is not necessarily the case.

24 Then the growth rate contributed by sulfuric acid during the time period used for the  
 25 determination of GR is calculated directly as:

1 
$$GR_{H_2SO_4} = [H_2SO_4]_{est} / C_{GR=1nm/h, H_2SO_4} \quad [14]$$

2 where  $[H_2SO_4]_{est}$  is the median value from the estimated sulfuric acid concentration during the  
3 timeframe for the determination of GR.

4 The observed growth rate can be presented as the sum of the growth rates due to  $H_2SO_4$   
5 ( $GR_{H_2SO_4}$ ) and organic vapors ( $GR_{org}$ ) condensation (Paasonen et al., 2010):

6 
$$GR_{obs} = GR_{H_2SO_4} + GR_{org} \quad [15]$$

7 By combining equations [13-15], the overall particle volume change can be separated into two  
8 fraction contributing by  $H_2SO_4$  and organic vapors condensation.

## 9 **4 Results**

### 10 **4.1 Particle formation and growth**

11 The previous study on the basis of long-term observations showed that the NPF events take place  
12 frequently at Melpitz, especially on April, May, and June (Hamed et al., 2010). During our field  
13 campaign (from May 23<sup>rd</sup> to June 8<sup>th</sup> in 2008), the NPF events were also observed frequently. In  
14 present study, three NPF events, which consecutively took place from June 5 to June 7, 2008, as  
15 displayed in Fig. 1 (a), are selected for further analysis. These events are the best cases which  
16 showed clear particle bursts and subsequent growth process during the entire field campaign. The  
17 starting and ending time for each event were marked in the Fig.1 (a) as NPF1, NPF2, and NPF3.  
18 The bursts in number concentration of 3-10 nm particles were observed associated with  
19 increasing ambient temperature, decreasing relative humidity (shown in Fig. 2 (b)), and  
20 increasing in estimated  $H_2SO_4$  concentration (shown in Fig. 1(b)). The CS is between 0.01 and  
21  $0.02 \text{ s}^{-1}$  during the NPF events. As marked in Fig.1 (a), the particle number size distribution  
22 shows the new particle formed around 10:00 a.m. and then grew with time for more than 20 h.  
23 This means that the NPF is a regional event (refer to Hussein et al., 2000) and could take place  
24 over a distance of a hundred kilometers. The Fig.2 (a) displays the wind speed and wind  
25 direction during the NPF events. The wind showed a typical diurnal cycle. The wind speed was  
26 4-5 m/s and kept a constant direction (south) during the daytime. It was static wind during  
27 nighttime. The particle formation rates ( $J_{3-25nm}$ ) were 13.5, 6.1, 9.3  $\text{cm}^{-3}\text{s}^{-1}$  on June 5, 6, and 7,

1 respectively. The highest formation rate was observed on June 5 corresponding to the highest  
2 H<sub>2</sub>SO<sub>4</sub> concentration.

3 As indicated by the white circle in the Fig.1 (a), the D<sub>m</sub> of log-normal ultrafine particle mode  
4 increased to around 100 nm within 24 hours. Over the time period from the beginning to the end  
5 of the NPF events as marked in Fig.1 (a), the average GR<sub>obs</sub>s were respectively 2.8, 3.6, and 4.4  
6 nm h<sup>-1</sup> for NPF events on June 5<sup>th</sup>, 6<sup>th</sup>, and 7<sup>th</sup>, 2008. One can note that the newly formed  
7 particles continued growing during the nighttime when sulfuric acid concentration was close to  
8 zero. This indicated that other species, most likely, organic compounds contributed to the particle  
9 growth during this time period.

10 There were no local emission sources in the surrounding areas of the Melpitz research station.  
11 The possible primary emissions contributing to the atmospheric particles at Melpitz could come  
12 from the cities, which are tens of kilometers away from the station. Typically, the primary  
13 particles are accompanied by trace gases, such as NO and SO<sub>2</sub> spikes. However, such  
14 phenomena were not observed in our measurements at Melpitz. As shown in Fig.2 (c), in the  
15 early morning on 6 and 7 June, the slight enhancement of NO (a tracer for traffic related ultrafine  
16 particles (Janhäll et al., 2004)) concentration may be caused by the outflow of cities nearby  
17 Melpitz. The particle number concentration did not increase simultaneously. The ultrafine  
18 particles exhausted from car tailpipes in the cities may grow by condensation and coagulation  
19 and shift towards larger diameters and diluted by fresh air significantly with increasing distance  
20 from the roads (Zhu et al., 2002). As a result, the enhancement in ultrafine particle number  
21 concentration was not observed at the rural site of Melpitz. Therefore, the instant impacts of  
22 primary emissions on atmospheric particles were not observed during the time period focused in  
23 this study. SO<sub>2</sub> from primary emissions could contribute to the atmospheric nucleation after  
24 being oxidized to sulfuric acid by radicals. The new particle formation associating with enhanced  
25 SO<sub>2</sub> concentration was observed by many previous studies (e.g. Birmili and Wiedensohler, 2000).  
26 Overall, the new particle formation and subsequent growth is the major source of particles, and  
27 thereby, CCN at Melpitz station.

## 28 **4.2 Hygroscopicity and chemical composition of newly formed particles**

29 Fig.3 displayed the size-resolved particle hygroscopicity (a), m/z 44 and 57 mass concentrations  
30 (b), and mass fraction of organic, sulfate, nitrate, and ammonium in 30-100 nm (mobility

1 diameter) particles (c). As shown in the Fig. 3(a), peak daily  $\kappa$ s of 50, 75, and 110 nm particles  
2 occurred afternoon and minimum appeared in the midnight. The evolution of particle  
3 hygroscopicity was very similar to those of inorganic mass fraction (sulfate+nitrate+ ammonium)  
4 in 30-100 nm particles. During the daytime,  $\text{H}_2\text{SO}_4$  concentration increased and may condense  
5 onto the particles. At the same time, the increasing ambient temperature (see Fig. 2 (b)) could  
6 drive the semi-volatile organic species in particle phase to partition to gas phase. Both processes  
7 could result in an enhanced inorganic mass fraction in particle phase, thereby enhancement in  
8 particle hygroscopicity. The decline in particle hygroscopicity took place after 15:30 (Local time)  
9 when sulfuric acid concentration decreased significantly. Simultaneously, ambient temperature  
10 decreased to an eventual nighttime minimum of around  $10^\circ\text{C}$ . Lower temperature facilitates the  
11 condensation of semi-volatile organic vapors onto the particles. As a result, the organic mass  
12 fraction increased significantly during the nighttime, as shown by AMS measurements (Fig.3 (c)),  
13 leading to an evident decline in particle hygroscopicity.

14 Table 3 summarizes the equivalent water-soluble fraction of newly formed particles when these  
15 particles grew to 35, 50, and 75 nm, respectively. Here, the equivalent water-soluble fraction is  
16 corresponding to the H-TDMA measurement points at which the  $D_m$  of ultrafine particle mode  
17 reached 35, 50, and 75 nm. On June 7, the equivalent water-soluble fraction of 35 nm newly  
18 formed particles was 34%. It decreased to 23% when particle grew to 50 nm, further, reduced to  
19 17% when particles reached to 75 nm. On June 5 and 6, the hygroscopicity of newly formed  
20 particles decreased with increasing particle size, as well. It implies that a large fraction of species  
21 contributing to particle growth was organics, which are typically less water soluble. This can be  
22 confirmed by AMS measurements showing that organic fraction in particles increased at a  
23 relatively later time of the NPF event (see Fig. 3(c)). The contribution of  $\text{H}_2\text{SO}_4$  condensation to  
24 particle growth was estimated using the method introduced in section 3.5 for different particle  
25 sizes. The ratios of  $\text{H}_2\text{SO}_4$  condensational growth to the observed particle growth ( $F_{\text{GR-H}_2\text{SO}_4}$   
26  $=\text{GR}_{\text{H}_2\text{SO}_4}/\text{GR}_{\text{obs}}$ ) are given in the table 3. For example, on June 7,  $F_{\text{GR-H}_2\text{SO}_4}$  was 30% for 35  
27 nm particles, meaning that  $\text{H}_2\text{SO}_4$  condensation only contributed 30% of the observed particle  
28 growth. With increasing particle size, the contribution of  $\text{H}_2\text{SO}_4$  condensation decreased, as  
29 shown in Table 3. This was consistent with the changes in the equivalent water-soluble fraction  
30 of newly formed particles. Both particle hygroscopicity measurements and numerical analysis  
31 showed that organics were potentially major contributors to the particle growth.

1 As displayed in Fig.3 (c), the organic compounds were dominating species in 30-100 nm  
2 particles in the particle formation period (indicated by grey dashed line). In this period, most of  
3 newly formed particles were smaller than 30 nm, as shown in Fig. 1 (a). They are too small to be  
4 detected by HR-Tof-AMS. Therefore, AMS measurements cannot provide proper information on  
5 chemical composition of newly formed particles in particle formation period. After around 12:00,  
6 the newly formed particles grew beyond 30 nm. Simultaneously, an obvious increase in sulfate  
7 and ammonium mass fraction in 30-100 nm particles was observed. This indicates that the newly  
8 formed particles were dominated by sulfate and ammonium. After 3:00 p.m., the organic mass  
9 fraction increased and reached its maximum at midnight on each day, indicating that organics  
10 played a key role in the particle growth at a later time of the NPF event. The mass fraction of ion  
11 fragments  $m/z$  44 and 57 in 30-100 nm particles are shown in the Fig. 3(b). The  $m/z$  44 ( $\text{CO}_2^+$   
12 ion fragment) is a tracer for secondary organic aerosol, while  $m/z$  57 ( $\text{C}_4\text{H}_9^+$ ) is generally  
13 associated with primary organics from combustion sources (Zhang et al., 2004a). The  $m/z$  57  
14 mass concentration was close to zero during the events. Compared  $m/z$  57, the  $m/z$  44 mass  
15 concentration were considerable, indicating that the organics contributing to particle growth was  
16 mainly secondary organic species.

### 17 **4.3 Enhancement in CCN number concentration during the NPF events**

18 The critical diameters and CCN number concentrations at different supersaturations during the  
19 NPF events are displayed in the Fig. 4. The critical diameters at different supersaturations  
20 decreased during the first several hours of the NPF events and enhanced at a later time of the  
21 NPF event. This was consistent with the variations in particle hygroscopic growth at  $\text{RH}=90\%$   
22 above-mentioned (see Fig. 3(a)). As shown in the Fig. 4(b), the CCN number concentration  
23 clearly increased significantly during the NPF events. The minimum in CCN number  
24 concentration was observed during the period of particle formation and the maximum appeared  
25 at the end of the NPF events.

26 The NPF events occurred on June 5, 6, and 7 were typical regional cases. The enhancement in  
27 CCN number concentration caused by atmospheric nucleation was evaluated by comparing the  
28 average CCN number concentrations over two hours prior to the beginning of the event (the  
29 period  $t_1$  marked in Fig. 4) with the same time period before the end of the events (the period  $t_2$   
30 marked in Fig. 4). The ratios of average CCN number concentration over  $t_2$  to  $t_1$  were

1 respectively 1.9, 2.0, and 1.5 for 0.1%, 0.4%, and 0.6% SS. On average, the enhancement ratios  
2 in CCN number concentration associated with individual NPF events were 63%, 66%, and 69%  
3 for 0.1, 0.4, and 0.6% SS, respectively. The absolute increases in CCN number concentrations  
4 associated with each event were 162, 931, and 756 #/cm<sup>3</sup>, on average.

5 Atmospheric boundary layer development and turbulent mixing will impact on NPF (Boy et al.,  
6 2006; Boy et al., 2003; Altstädter et al., 2015), and consequently on its CCN products. It is hard  
7 task to quantify the changes in CCN number due to boundary layer dynamics. In this study, the  
8 enhancement in CCN number concentration caused by atmospheric nucleation was evaluated by  
9 a ratio of CCN number during the same period on different days, and not an absolute value. Here  
10 we assume that the weather condition and boundary layer height were similar during two time  
11 periods (see meteorological parameters in Fig. 3). Therefore, we assumed that the effect of  
12 boundary layer dynamics on the change in CCN number concentration could be ignored.

13 Several previous studies reported that the enhancement in CCN number concentration associated  
14 with atmospheric nucleation varied significantly in different environments. At the Finnish sub-  
15 Arctic Pallas station, a 210±110% increase in the number concentration of 80 nm particles was  
16 observed from the beginning of a nucleation event to the end of the event (Asmi et al., 2011). At  
17 a forested site (SMEAR II station in Hyytiälä) in Southern Finland, nucleation enhanced CCN  
18 number concentration by 70 to 110%, varying with the supersaturation level (Sihto et al., 2011).  
19 In a polluted urban area, Beijing, China, the average CCN enhancement factors were between  
20 about 1.5 and 2.5 (Yue et al., 2011; Wiedensohler et al., 2009). In Boulder, CO, Atlanta, GA, and  
21 Tecamac, Mexico, the pre-existing CCN number concentration increased on average by a factor  
22 of 3.8 as a result of new particle formation (Kuang et al., 2009). Overall, the enhancement in  
23 CCN number concentration associated with atmospheric nucleation varied significantly in  
24 different environments. Please note that the methods for defining the enhancement factors used  
25 in the existing literature were very different. Therefore, a general conclusion on how significant  
26 NPF and growth process contributes to CCN budget cannot be drawn, currently.

## 27 **5 Discussion**

28 The above field observations clearly showed that newly formed particles had the ability to grow  
29 into CCN sizes within several hours at Melpitz. The particle hygroscopicity measurements  
30 strongly suggested that organic compounds were the major contributors driving particle growth

1 into CCN sizes. The previous studies performed in clean atmosphere also showed that the newly  
2 formed particles mainly consist of organics. For examples, sulfuric acid is able to account for  
3 roughly 30% of the growth rate of newly formed particles in the rural atmosphere of  
4 Hohenpeissenberg, Southern Germany (Birmili et al., 2003), and only around 10% in the boreal  
5 forest area of Finland (Boy et al., 2005). However, In the polluted atmosphere of Atlanta, USA,  
6 the available amount of sulfuric acid was sufficient to explain all of the observed particle growth  
7 (Stolzenburg et al., 2005). At Melpitz, biogenic volatile organic compounds (BVOCs) emitted  
8 from biological activities are dominating volatile organic compounds (Mutzel et al., 2015) and  
9 lead to an organic-rich environment during the summertime. The oxidation products of BVOCs  
10 may be responsible for the new particle growth.

11 We note that the condensation of organics lead to a rapid particle growth when sulfuric acid  
12 concentration was close to zero during the nighttime, as shown in Fig. 1. The organic condensing  
13 materials with low hygroscopicity reduced CCN efficiency of the new particles, as indicated by  
14 critical diameters given in Fig. 4. Such phenomenon was also reported by Dusek et al. (2010).  
15 They showed that enhanced organic mass fraction caused a reduction in CCN efficiency of small  
16 particles during the new particle formation. These results implied that the CCN production  
17 associated with atmospheric nucleation may be overestimated if assuming that new particles can  
18 serve as CCN in case they grow to a fixed particle size (Such as Asmi et al., 2011), especially for  
19 organic-rich environments. In our case, the mean critical diameter is around 50 nm at SS=0.6%.  
20 Assuming a constant critical diameter of 50 nm at SS=0.6%, the CCN number concentration was  
21 averagely 1.13 times of that with varied critical diameters during the NPF events. Under similar  
22 conditions, the CCN number concentration at SS=0.4% with a constant critical diameter of 70  
23 nm was 1.15 times of that with varied critical diameters.

## 24 **6 Conclusions**

25 In this study, the particle number size distribution, particle hygroscopicity, and particle chemical  
26 composition during three regional NPF events were measured to investigate the new particle  
27 growth process and its effects on CCN activity. The particle formation rates ( $J_{3-25\text{nm}}$ ) were 13.5,  
28 6.1, 9.3  $\text{cm}^{-3}\text{s}^{-1}$ , and the particle growth rates were 2.8, 3.6, and 4.4 nm/h for NPF events on June  
29 5, 6 and 7, 2008, respectively.

1 The  $(\text{NH}_4)_2\text{SO}_4$ -equivalent water-soluble fraction accounted for 20% and 16% of 50 and 75 nm  
2 newly formed particles, respectively. AMS measurements showed that the sulfate and  
3 ammonium were dominating chemical species when newly formed particles grew beyond 30 nm  
4 shortly after particle formation period. At a later time of NPF event, the organics played a key  
5 role in the particle growth. The analysis on the fragment  $m/z$  44 and 57 showed that the organics  
6 contributing to particle growth was mainly secondary organic species. The particle  
7 hygroscopicity and chemical composition measurements and numerical calculation confirmed  
8 that organic compounds were major contributors driving particles growth to CCN sizes.

9 The step-wised increase in CCN number concentration during three consecutive NPF events was  
10 observed. On average, the enhancement ratios in CCN number concentration associated with  
11 individual NPF events are 63%, 66%, 69% for 0.1, 0.4, and 0.6% SS, respectively. We found  
12 that the new particles hygroscopicity decreased significantly with condensational growth of  
13 organic compounds, which are generally less water soluble. Correspondingly, the critical  
14 diameters at a certain supersaturation increased, indicating that enhanced organic mass fraction  
15 caused a reduction in CCN efficiency of newly formed particles during the new particle  
16 formation. Our results implied that the CCN production associated with atmospheric nucleation  
17 may be overestimated if assuming that new particles can serve as CCN in case they grow to a  
18 fixed particle size, which was used in some previous studies, especially for organic-rich  
19 environments.

## 20 **Acknowledgements**

21 The data analysis work done by the first author is supported by National Natural Science  
22 Foundation of China (41475127). Data collection was supported by the European Commission  
23 projects EUSAAR (European Supersites for Atmospheric Aerosol Research), EUCAARI  
24 (European Integrated project on Aerosol Cloud Climate and Air Quality Interactions) FP6-  
25 036833-2-EUCAARI, and the German Federal Environment Ministry (BMU) grant F&E  
26 370343200. We acknowledge Friederike Kinder, Andreas Maßling, and Thomas Tuch for their  
27 contributions related to H-TDMA and TDMPS data acquisition.

28

29



1

2

### 3 **References**

- 4 Altstädter, B., Platis, A., Wehner, B., Scholtz, A., Wildmann, N., Hermann, M., Käthner, R., Baars, H.,  
5 Bange, J., and Lampert, A.: ALADINA – an unmanned research aircraft for observing vertical and  
6 horizontal distributions of ultrafine particles within the atmospheric boundary layer, *Atmos. Meas. Tech.*,  
7 8, 1627-1639, 10.5194/amt-8-1627-2015, 2015.
- 8 Asmi, E., Kivekäs, N., Kerminen, V. M., Komppula, M., Hyvärinen, A. P., Hatakka, J., Viisanen, Y., and  
9 Lihavainen, H.: Secondary new particle formation in Northern Finland Pallas site between the years 2000  
10 and 2010, *Atmos. Chem. Phys.*, 11, 12959-12972, 10.5194/acp-11-12959-2011, 2011.
- 11 Birmili, W., Stratmann, F., and Wiedensohler, A.: Design of a DMA-based size spectrometer for a large  
12 particle size range and stable operation, *J. Aerosol Sci.*, 30, 549-553, 1999.
- 13 Birmili, W., and Wiedensohler, A.: New particle formation in the continental boundary layer:  
14 Meteorological and gas phase parameter influence, *Geophysical Research Letters*, 27, 3325-3328,  
15 10.1029/1999GL011221, 2000.
- 16 Birmili, W., Berresheim, H., Plass-Dülmer, C., Elste, T., Gilge, S., Wiedensohler, A., and Uhrner, U.: The  
17 Hohenpeissenberg aerosol formation experiment (HAFEX): a long-term study including size-resolved  
18 aerosol, H<sub>2</sub>SO<sub>4</sub>, OH, and monoterpenes measurements, *Atmos. Chem. Phys.*, 3, 361-376, 10.5194/acp-3-  
19 361-2003, 2003.
- 20 Birmili, W., Weinhold, K., Nordmann, S., Wiedensohler, A., Spindler, G., Müller, K., Herrmann, H.,  
21 Gnauk, T., Pitz, M., Cyrys, J., Flentje, H., Nickel, C., Kuhlbusch, T. A. J., and Löschau, G.: Atmospheric  
22 aerosol measurements in the German Ultrafine Aerosol Network (GUAN): Part 1 - soot and particle  
23 number size distribution, *Gefahrst. Reinh. Luft.*, 69, 137-145, 2009.
- 24 Boy, M., Rannik, Ü., Lehtinen, K. E. J., Tarvainen, V., Hakola, H., and Kulmala, M.: Nucleation events  
25 in the continental boundary layer: Long-term statistical analyses of aerosol relevant characteristics,  
26 *Journal of Geophysical Research: Atmospheres*, 108, n/a-n/a, 10.1029/2003JD003838, 2003.
- 27 Boy, M., Kulmala, M., Ruuskanen, T. M., Pihlatie, M., Reissell, A., Aalto, P. P., Keronen, P., Dal Maso,  
28 M., Hellen, H., Hakola, H., Jansson, R., Hanke, M., and Arnold, F.: Sulphuric acid closure and  
29 contribution to nucleation mode particle growth, *Atmos. Chem. Phys.*, 5, 863-878, 10.5194/acp-5-863-  
30 2005, 2005.
- 31 Boy, M., Hellmuth, O., Korhonen, H., Nilsson, E. D., ReVelle, D., Turnipseed, A., Arnold, F., and  
32 Kulmala, M.: MALTE – model to predict new aerosol formation in the lower troposphere, *Atmos.*  
33 *Chem. Phys.*, 6, 4499-4517, 10.5194/acp-6-4499-2006, 2006.

- 1 Brus, D., Neitola, K., Hyvärinen, A. P., Petäjä, T., Vanhanen, J., Sipilä, M., Paasonen, P., Kulmala, M.,  
2 and Lihavainen, H.: Homogenous nucleation of sulfuric acid and water at close to atmospherically  
3 relevant conditions, *Atmos. Chem. Phys.*, 11, 5277-5287, 10.5194/acp-11-5277-2011, 2011.
- 4 Canagaratna, M. R., Jayne, J. T., Jimenez, J. L., Allan, J. D., Alfarra, M. R., Zhang, Q., Onasch, T. B.,  
5 Drewnick, F., Coe, H., Middlebrook, A., Delia, A., Williams, L. R., Trimborn, A. M., Northway, M. J.,  
6 DeCarlo, P. F., Kolb, C. E., Davidovits, P., and Worsnop, D. R.: Chemical and microphysical  
7 characterization of ambient aerosols with the aerodyne aerosol mass spectrometer, *Mass Spectrometry*  
8 *Reviews*, 26, 185-222, 10.1002/mas.20115, 2007.
- 9 Cerully, K. M., Raatikainen, T., Lance, S., Tkacik, D., Tiitta, P., Petäjä, T., Ehn, M., Kulmala, M.,  
10 Worsnop, D. R., Laaksonen, A., Smith, J. N., and Nenes, A.: Aerosol hygroscopicity and CCN activation  
11 kinetics in a boreal forest environment during the 2007 EUCAARI campaign, *Atmos. Chem. Phys.*, 11,  
12 12369-12386, 10.5194/acp-11-12369-2011, 2011.
- 13 Dal Maso, M., Kulmala, M., Riipinen, I., Wagner, R., Hussein, T., Aalto, P. P., and Lehtinen, K. E.:  
14 Formation and growth of fresh atmospheric aerosols: eight years of aerosol size distribution data from  
15 SMEAR II, Hyytiälä, Finland, *Boreal Environment Research*, 10, 323, 2005.
- 16 DeCarlo, P. F., Kimmel, J. R., Trimborn, A., Northway, M. J., Jayne, J. T., Aiken, A. C., Gonin, M.,  
17 Fuhrer, K., Horvath, T., Docherty, K. S., Worsnop, D. R., and Jimenez, J. L.: Field-Deployable, High-  
18 Resolution, Time-of-Flight Aerosol Mass Spectrometer, *Analytical Chemistry*, 78, 8281-8289,  
19 10.1021/ac061249n, 2006.
- 20 Dusek, U., Frank, G. P., Hildebrandt, L., Curtius, J., Schneider, J., Walter, S., Chand, D., Drewnick, F.,  
21 Hings, S., Jung, D., Borrmann, S., and Andreae, M. O.: Size Matters More Than Chemistry for Cloud-  
22 Nucleating Ability of Aerosol Particles, *Science*, 312, 1375-1378, 10.1126/science.1125261, 2006.
- 23 Dusek, U., Frank, G. P., Curtius, J., Drewnick, F., Schneider, J., Kürten, A., Rose, D., Andreae, M. O.,  
24 Borrmann, S., and Pöschl, U.: Enhanced organic mass fraction and decreased hygroscopicity of cloud  
25 condensation nuclei (CCN) during new particle formation events, *Geophysical Research Letters*, 37, n/a-  
26 n/a, 10.1029/2009GL040930, 2010.
- 27 Ehn, M., Petäjä, T., Aufmhoff, H., Aalto, P., Hämeri, K., Arnold, F., Laaksonen, A., and Kulmala, M.:  
28 Hygroscopic properties of ultrafine aerosol particles in the boreal forest: diurnal variation, solubility and  
29 the influence of sulfuric acid, *Atmos. Chem. Phys.*, 7, 211-222, 10.5194/acp-7-211-2007, 2007.
- 30 Good, N., Topping, D. O., Allan, J. D., Flynn, M., Fuentes, E., Irwin, M., Williams, P. I., Coe, H., and  
31 McFiggans, G.: Consistency between parameterisations of aerosol hygroscopicity and CCN activity  
32 during the RHAMBLE discovery cruise, *Atmos. Chem. Phys.*, 10, 3189-3203, 10.5194/acp-10-3189-2010,  
33 2010.
- 34 Größ, J., Birmili, W., Hamed, A., Sonntag, A., Wiedensohler, A., Spindler, G., Maninnen, H. E.,  
35 Nieminen, T., Kulmala, M., Hörrak, U., and Plass-Dülmer, C.: Evolution of gaseous precursors and  
36 meteorological parameters during new particle formation events in the Central European boundary layer,  
37 *Atmos. Chem. Phys. Discuss.*, 15, 2305-2353, 10.5194/acpd-15-2305-2015, 2015.

- 1 Gysel, M., Crosier, J., Topping, D. O., Whitehead, J. D., Bower, K. N., Cubison, M. J., Williams, P. I.,  
2 Flynn, M. J., McFiggans, G. B., and Coe, H.: Closure study between chemical composition and  
3 hygroscopic growth of aerosol particles during TORCH2, *Atmos. Chem. Phys.*, 7, 6131-6144,  
4 10.5194/acp-7-6131-2007, 2007.
- 5 Gysel, M., McFiggans, G. B., and Coe, H.: Inversion of tandem differential mobility analyser (TDMA)  
6 measurements, *Journal of Aerosol Science*, 40, 134-151, 10.1016/j.jaerosci.2008.07.013, 2009.
- 7 Hämeri, K., Väkevä, M., Aalto, P. P., Kulmala, M., Swietlicki, E., Zhou, J., Seidl, W., Becker, E., and  
8 O'Dowd, C. D.: Hygroscopic and CCN properties of aerosol particles in boreal forests, *Tellus B*, 53, 359-  
9 379, 10.1034/j.1600-0889.2001.530404.x, 2001.
- 10 Hamed, A., Birmili, W., Joutsensaari, J., Mikkonen, S., Asmi, A., Wehner, B., Spindler, G., Jaatinen, A.,  
11 Wiedensohler, A., Korhonen, H., Lehtinen, K. E. J., and Laaksonen, A.: Changes in the production rate of  
12 secondary aerosol particles in Central Europe in view of decreasing SO<sub>2</sub> emissions between 1996 and  
13 2006, *Atmos. Chem. Phys.*, 10, 1071-1091, 10.5194/acp-10-1071-2010, 2010.
- 14 Heintzenberg, J.: Properties of the Log-Normal Particle Size Distribution, *Aerosol Science and*  
15 *Technology*, 21, 46-48, 10.1080/02786829408959695, 1994.
- 16 Hussein, T., Aalto, P. P., and Lehtinen, K. E. J.: Formation and growth of fresh atmospheric aerosols:  
17 eight years of aerosol size distribution data from SMEAR II, Hyytiälä, Finland, 2000.
- 18 Irwin, M., Good, N., Crosier, J., Choularton, T. W., and McFiggans, G.: Reconciliation of measurements  
19 of hygroscopic growth and critical supersaturation of aerosol particles in central Germany, *Atmos. Chem.*  
20 *Phys.*, 10, 11737-11752, 10.5194/acp-10-11737-2010, 2010.
- 21 Janhäll, S., M. Jonsson, Å., Molnár, P., A. Svensson, E., and Hallquist, M.: Size resolved traffic emission  
22 factors of submicrometer particles, *Atmospheric Environment*, 38, 4331-4340,  
23 <http://dx.doi.org/10.1016/j.atmosenv.2004.04.018>, 2004.
- 24 Kazil, J., Stier, P., Zhang, K., Quaas, J., Kinne, S., O'Donnell, D., Rast, S., Esch, M., Ferrachat, S.,  
25 Lohmann, U., and Feichter, J.: Aerosol nucleation and its role for clouds and Earth's radiative forcing in  
26 the aerosol-climate model ECHAM5-HAM, *Atmos. Chem. Phys.*, 10, 10733-10752, 10.5194/acp-10-  
27 10733-2010, 2010.
- 28 Kerminen, V.-M., Lehtinen, K. E. J., Anttila, T., and Kulmala, M.: Dynamics of atmospheric nucleation  
29 mode particles: a timescale analysis, *Tellus B*, 56, 135-146, 10.3402/tellusb.v56i2.16411, 2004.
- 30 Kerminen, V. M., Paramonov, M., Anttila, T., Riipinen, I., Fountoukis, C., Korhonen, H., Asmi, E.,  
31 Laakso, L., Lihavainen, H., Swietlicki, E., Svenningsson, B., Asmi, A., Pandis, S. N., Kulmala, M., and  
32 Petäjä, T.: Cloud condensation nuclei production associated with atmospheric nucleation: a synthesis  
33 based on existing literature and new results, *Atmos. Chem. Phys.*, 12, 12037-12059, 10.5194/acp-12-  
34 12037-2012, 2012.

- 1 Kiendler-Scharr, A., Wildt, J., Maso, M. D., Hohaus, T., Kleist, E., Mentel, T. F., Tillmann, R., Uerlings,  
2 R., Schurr, U., and Wahner, A.: New particle formation in forests inhibited by isoprene emissions, *Nature*,  
3 461, 381-384, [http://www.nature.com/nature/journal/v461/n7262/supinfo/nature08292\\_S1.html](http://www.nature.com/nature/journal/v461/n7262/supinfo/nature08292_S1.html), 2009.
- 4 Kuang, C., McMurry, P. H., and McCormick, A. V.: Determination of cloud condensation nuclei  
5 production from measured new particle formation events, *Geophysical Research Letters*, 36, L09822,  
6 10.1029/2009GL037584, 2009.
- 7 Kulmala, M., Laakso, L., Lehtinen, K. E. J., Riipinen, I., Dal Maso, M., Anttila, T., Kerminen, V. M.,  
8 Hörrak, U., Vana, M., and Tammet, H.: Initial steps of aerosol growth, *Atmos. Chem. Phys.*, 4, 2553-  
9 2560, 10.5194/acp-4-2553-2004, 2004.
- 10 Kulmala, M., Lehtinen, K. E. J., and Laaksonen, A.: Cluster activation theory as an explanation of the  
11 linear dependence between formation rate of 3nm particles and sulphuric acid concentration, *Atmos.*  
12 *Chem. Phys.*, 6, 787-793, 10.5194/acp-6-787-2006, 2006.
- 13 Kulmala, M., Asmi, A., Lappalainen, H. K., Carslaw, K. S., Pöschl, U., Baltensperger, U., Hov, Ø.,  
14 Brenquier, J. L., Pandis, S. N., Facchini, M. C., Hansson, H. C., Wiedensohler, A., and O'Dowd, C. D.:  
15 Introduction: European Integrated Project on Aerosol Cloud Climate and Air Quality interactions  
16 (EUCAARI) – integrating aerosol research from nano to global scales, *Atmos. Chem. Phys.*, 9, 2825-  
17 2841, 10.5194/acp-9-2825-2009, 2009.
- 18 Kulmala, M., Petäjä, T., Nieminen, T., Sipilä, M., Manninen, H. E., Lehtipalo, K., Dal Maso, M., Aalto, P.,  
19 P., Junninen, H., Paasonen, P., Riipinen, I., Lehtinen, K. E. J., Laaksonen, A., and Kerminen, V.-M.:  
20 Measurement of the nucleation of atmospheric aerosol particles, *Nat. Protocols*, 7, 1651-1667,  
21 <http://www.nature.com/nprot/journal/v7/n9/abs/nprot.2012.091.html#supplementary-information>, 2012.
- 22 Kurtén, T., Torpo, L., Ding, C.-G., Vehkamäki, H., Sundberg, M. R., Laasonen, K., and Kulmala, M.: A  
23 density functional study on water-sulfuric acid-ammonia clusters and implications for atmospheric cluster  
24 formation, *Journal of Geophysical Research: Atmospheres*, 112, n/a-n/a, 10.1029/2006jd007391, 2007.
- 25 Laakso, L., Petäjä, T., Lehtinen, K. E. J., Kulmala, M., Paatero, J., Hörrak, U., Tammet, H., and  
26 Joutsensaari, J.: Ion production rate in a boreal forest based on ion, particle and radiation measurements,  
27 *Atmos. Chem. Phys.*, 4, 1933-1943, 10.5194/acp-4-1933-2004, 2004.
- 28 Laakso, L., Merikanto, J., Vakkari, V., Laakso, H., Kulmala, M., Molefe, M., Kgabi, N., Mabaso, D.,  
29 Carslaw, K. S., Spracklen, D. V., Lee, L. A., Reddington, C. L., and Kerminen, V. M.: Boundary layer  
30 nucleation as a source of new CCN in savannah environment, *Atmos. Chem. Phys.*, 13, 1957-1972,  
31 10.5194/acp-13-1957-2013, 2013.
- 32 Laaksonen, A., Hamed, A., Joutsensaari, J., Hiltunen, L., Cavalli, F., Junkermann, W., Asmi, A., Fuzzi, S.,  
33 and Facchini, M. C.: Cloud condensation nucleus production from nucleation events at a highly polluted  
34 region, *Geophys. Res. Lett.*, 32, L06812, 10.1029/2004gl022092, 2005.

- 1 Malm, W. C., and Kreidenweis, S. M.: The effects of models of aerosol hygroscopicity on the  
2 apportionment of extinction, *Atmospheric Environment*, 31, 1965-1976, 10.1016/s1352-2310(96)00355-x,  
3 1997.
- 4 Massling, A., Wiedensohler, A., Busch, B., Neusüß, C., Quinn, P., Bates, T., and Covert, D.: Hygroscopic  
5 properties of different aerosol types over the Atlantic and Indian Oceans, *Atmos. Chem. Phys.*, 3, 1377-  
6 1397, 10.5194/acp-3-1377-2003, 2003.
- 7 Massling, A., Niedermeier, N., Hennig, T., Fors, E. O., Swietlicki, E., Ehn, M., Hämeri, K., Villani, P.,  
8 Laj, P., Good, N., McFiggans, G., and Wiedensohler, A.: Results and recommendations from an  
9 intercomparison of six Hygroscopicity-TDMA systems, *Atmos. Meas. Tech.*, 4, 485-497, 10.5194/amt-4-  
10 485-2011, 2011.
- 11 Merikanto, J., Spracklen, D. V., Mann, G. W., Pickering, S. J., and Carslaw, K. S.: Impact of nucleation  
12 on global CCN, *Atmos. Chem. Phys.*, 9, 8601-8616, 10.5194/acp-9-8601-2009, 2009.
- 13 Mutzel, A., Poulain, L., Berndt, T., Iinuma, Y., Rodigast, M., Böge, O., Richters, S., Spindler, G., Sipilä,  
14 M., Jokinen, T., Kulmala, M., and Herrmann, H.: Highly Oxidized Multifunctional Organic Compounds  
15 Observed in Tropospheric Particles: A Field and Laboratory Study, *Environmental Science & Technology*,  
16 49, 7754-7761, 10.1021/acs.est.5b00885, 2015.
- 17 Nieminen, T., Lehtinen, K. E. J., and Kulmala, M.: Sub-10 nm particle growth by vapor condensation –  
18 effects of vapor molecule size and particle thermal speed, *Atmos. Chem. Phys.*, 10, 9773-9779,  
19 10.5194/acp-10-9773-2010, 2010.
- 20 Paasonen, P., Nieminen, T., Asmi, E., Manninen, H. E., Petäjä, T., Plass-Dülmer, C., Flentje, H., Birmili,  
21 W., Wiedensohler, A., Hörrak, U., Metzger, A., Hamed, A., Laaksonen, A., Facchini, M. C., Kerminen, V.  
22 M., and Kulmala, M.: On the roles of sulphuric acid and low-volatility organic vapours in the initial steps  
23 of atmospheric new particle formation, *Atmos. Chem. Phys.*, 10, 11223-11242, 10.5194/acp-10-11223-  
24 2010, 2010.
- 25 Paasonen, P., Asmi, A., Petaja, T., Kajos, M. K., Aijala, M., Junninen, H., Holst, T., Abbatt, J. P. D.,  
26 Arneth, A., Birmili, W., van der Gon, H. D., Hamed, A., Hoffer, A., Laakso, L., Laaksonen, A., Richard  
27 Leaitch, W., Plass-Dulmer, C., Pryor, S. C., Raisanen, P., Swietlicki, E., Wiedensohler, A., Worsnop, D.  
28 R., Kerminen, V.-M., and Kulmala, M.: Warming-induced increase in aerosol number concentration  
29 likely to moderate climate change, *Nature Geosci*, 6, 438-442, 10.1038/ngeo1800  
30 <http://www.nature.com/ngeo/journal/v6/n6/abs/ngeo1800.html#supplementary-information>, 2013.
- 31 Petters, M. D., and Kreidenweis, S. M.: A single parameter representation of hygroscopic growth and  
32 cloud condensation nucleus activity, *Atmos. Chem. Phys.*, 7, 1961-1971, 10.5194/acp-7-1961-2007, 2007.
- 33 Petters, M. D., Wex, H., Carrico, C. M., Hallbauer, E., Massling, A., McMeeking, G. R., Poulain, L., Wu,  
34 Z., Kreidenweis, S. M., and Stratmann, F.: Towards closing the gap between hygroscopic growth and  
35 activation for secondary organic aerosol – Part 2: Theoretical approaches, *Atmos. Chem. Phys.*, 9, 3999-  
36 4009, 10.5194/acp-9-3999-2009, 2009.

- 1 Pierce, J. R., Riipinen, I., Kulmala, M., Ehn, M., Petäjä, T., Junninen, H., Worsnop, D. R., and Donahue,  
2 N. M.: Quantification of the volatility of secondary organic compounds in ultrafine particles during  
3 nucleation events, *Atmos. Chem. Phys.*, 11, 9019-9036, 10.5194/acp-11-9019-2011, 2011.
- 4 Pirjola, L., Kulmala, M., Wilck, M., Bischoff, A., Stratmann, F., and Otto, E.: FORMATION OF  
5 SULPHURIC ACID AEROSOLS AND CLOUD CONDENSATION NUCLEI: AN EXPRESSION FOR  
6 SIGNIFICANT NUCLEATION AND MODEL COMPARISON, *Journal of Aerosol Science*, 30, 1079-  
7 1094, [http://dx.doi.org/10.1016/S0021-8502\(98\)00776-9](http://dx.doi.org/10.1016/S0021-8502(98)00776-9), 1999.
- 8 Potukuchi, S., and Wexler, A. S.: Identifying solid-aqueous phase transitions in atmospheric aerosols—I.  
9 Neutral-acidity solutions, *Atmospheric Environment*, 29, 1663-1676, [http://dx.doi.org/10.1016/1352-  
10 2310\(95\)00074-9](http://dx.doi.org/10.1016/1352-2310(95)00074-9), 1995.
- 11 Poulain, L., Birmili, W., Canonaco, F., Crippa, M., Wu, Z. J., Nordmann, S., Spindler, G., Prévôt, A. S.  
12 H., Wiedensohler, A., and Herrmann, H.: Chemical mass balance of 300 °C non-volatile particles at the  
13 tropospheric research site Melpitz, Germany, *Atmos. Chem. Phys.*, 14, 10145-10162, 10.5194/acp-14-  
14 10145-2014, 2014.
- 15 Ristovski, Z. D., Suni, T., Kulmala, M., Boy, M., Meyer, N. K., Duplissy, J., Turnipseed, A., Morawska,  
16 L., and Baltensperger, U.: The role of sulphates and organic vapours in growth of newly formed particles  
17 in a eucalypt forest, *Atmos. Chem. Phys.*, 10, 2919-2926, 10.5194/acp-10-2919-2010, 2010.
- 18 Sihto, S. L., Mikkilä, J., Vanhanen, J., Ehn, M., Liao, L., Lehtipalo, K., Aalto, P. P., Duplissy, J., Petäjä,  
19 T., Kerminen, V. M., Boy, M., and Kulmala, M.: Seasonal variation of CCN concentrations and aerosol  
20 activation properties in boreal forest, *Atmos. Chem. Phys.*, 11, 13269-13285, 10.5194/acp-11-13269-2011,  
21 2011.
- 22 Sipilä, M., Berndt, T., Petäjä, T., Brus, D., Vanhanen, J., Stratmann, F., Patokoski, J., Mauldin, R. L.,  
23 Hyvärinen, A.-P., Lihavainen, H., and Kulmala, M.: The Role of Sulfuric Acid in Atmospheric  
24 Nucleation, *Science*, 327, 1243-1246, 2010.
- 25 Smith, J. N., Moore, K. F., McMurry, P. H., and Eisele, F. L.: Atmospheric Measurements of Sub-20 nm  
26 Diameter Particle Chemical Composition by Thermal Desorption Chemical Ionization Mass Spectrometry,  
27 *Aerosol Science and Technology*, 38, 100-110, 10.1080/02786820490249036, 2004.
- 28 Sotiropoulou, R. E. P., Tagaris, E., Pilinis, C., Anttila, T., and Kulmala, M.: Modeling New Particle  
29 Formation During Air Pollution Episodes: Impacts on Aerosol and Cloud Condensation Nuclei, *Aerosol  
30 Science and Technology*, 40, 557-572, 10.1080/02786820600714346, 2006.
- 31 Spracklen, D. V., Carslaw, K. S., Kulmala, M., Kerminen, V.-M., Sihto, S.-L., Riipinen, I., Merikanto, J.,  
32 Mann, G. W., Chipperfield, M. P., Wiedensohler, A., Birmili, W., and Lihavainen, H.: Contribution of  
33 particle formation to global cloud condensation nuclei concentrations, *Geophys. Res. Lett.*, 35, L06808,  
34 10.1029/2007gl033038, 2008.
- 35 Stokes, R. H., and Robinson, R. A.: Interactions in Aqueous Nonelectrolyte Solutions. I. Solute-Solvent  
36 Equilibria, *Journal of Physical Chemistry*, 70, 2126-2130, 1966.

- 1 Stolzenburg, M. R., McMurry, P. H., Sakurai, H., Smith, J. N., Mauldin, R. L., Eisele, F. L., and Clement,  
2 C. F.: Growth rates of freshly nucleated atmospheric particles in Atlanta, *Journal of Geophysical*  
3 *Research: Atmospheres*, 110, D22S05, 10.1029/2005JD005935, 2005.
- 4 Swietlicki, E., Zhou, J., Berg, O. H., Martinsson, B. G., Frank, G., Cederfelt, S.-I., Dusek, U., Berner, A.,  
5 Birmili, W., Wiedensohler, A., Yuskiewicz, B., and Bower, K. N.: A closure study of sub-micrometer  
6 aerosol particle hygroscopic behaviour, *Atmospheric Research*, 50, 205-240, 10.1016/s0169-  
7 8095(98)00105-7, 1999.
- 8 Tang, I. N., and Munkelwitz, H. R.: Water activities, densities, and refractive indices of aqueous sulfates  
9 and sodium nitrate droplets of atmospheric importance, *J. Geophys. Res.*, 99, 18801-18808,  
10 10.1029/94jd01345, 1994.
- 11 Tuch, T. M., Haudek, A., Müller, T., Nowak, A., Wex, H., and Wiedensohler, A.: Design and  
12 performance of an automatic regenerating adsorption aerosol dryer for continuous operation at monitoring  
13 sites, *Atmos. Meas. Tech.*, 2, 417-422, 2009.
- 14 Varutbangkul, V., Brechtel, F. J., Bahreini, R., Ng, N. L., Keywood, M. D., Kroll, J. H., Flagan, R. C.,  
15 Seinfeld, J. H., Lee, A., and Goldstein, A. H.: Hygroscopicity of secondary organic aerosols formed by  
16 oxidation of cycloalkenes, monoterpenes, sesquiterpenes, and related compounds, *Atmos. Chem. Phys.*, 6,  
17 2367-2388, 10.5194/acp-6-2367-2006, 2006.
- 18 Virkkula, A., Van Dingenen, R., Raes, F., and Hjorth, J.: Hygroscopic properties of aerosol formed by  
19 oxidation of limonene,  $\alpha$ -pinene, and  $\beta$ -pinene, *J. Geophys. Res.*, 104, 3569-3579, 10.1029/1998jd100017,  
20 1999.
- 21 Wang, L., Khalizov, A. F., Zheng, J., Xu, W., Ma, Y., Lal, V., and Zhang, R.: Atmospheric nanoparticles  
22 formed from heterogeneous reactions of organics, *Nature Geosci.*, 3, 238-242,  
23 [http://www.nature.com/ngeo/journal/v3/n4/supinfo/ngeo778\\_S1.html](http://www.nature.com/ngeo/journal/v3/n4/supinfo/ngeo778_S1.html), 2010.
- 24 Wang, M., and Penner, J. E.: Aerosol indirect forcing in a global model with particle nucleation, *Atmos.*  
25 *Chem. Phys.*, 9, 239-260, 10.5194/acp-9-239-2009, 2009.
- 26 Weber, R. J., Marti, J. J., McMurry, P. H., Eisele, F. L., Tanner, D. J., and Jefferson, A.: Measurements of  
27 new particle formation and ultrafine particle growth rates at a clean continental site, *Journal of*  
28 *Geophysical Research: Atmospheres*, 102, 4375-4385, 10.1029/96JD03656, 1997.
- 29 Westervelt, D. M., Pierce, J. R., and Adams, P. J.: Analysis of feedbacks between nucleation rate, survival  
30 probability and cloud condensation nuclei formation, *Atmos. Chem. Phys.*, 14, 5577-5597, 10.5194/acp-  
31 14-5577-2014, 2014.
- 32 Wex, H., Petters, M. D., Carrico, C. M., Hallbauer, E., Massling, A., McMeeking, G. R., Poulain, L., Wu,  
33 Z., Kreidenweis, S. M., and Stratmann, F.: Towards closing the gap between hygroscopic growth and  
34 activation for secondary organic aerosol: Part 1 – Evidence from measurements, *Atmos. Chem. Phys.*, 9,  
35 3987-3997, 10.5194/acp-9-3987-2009, 2009.



- 1 Wiedensohler, A., Cheng, Y. F., Nowak, A., Wehner, B., Achtert, P., Berghof, M., Birmili, W., Wu, Z. J.,  
2 Hu, M., Zhu, T., Takegawa, N., Kita, K., Kondo, Y., Lou, S. R., Hofzumahaus, A., Holland, F., Wahner,  
3 A., Gunthe, S. S., Rose, D., Su, H., and Pöschl, U.: Rapid aerosol particle growth and increase of cloud  
4 condensation nucleus activity by secondary aerosol formation and condensation: A case study for regional  
5 air pollution in northeastern China, *J. Geophys. Res.*, 114, D00G08, 10.1029/2008jd010884, 2009.
- 6 Wiedensohler, A., Birmili, W., Nowak, A., Sonntag, A., Weinhold, K., Merkel, M., Wehner, B., Tuch, T.,  
7 Pfeifer, S., Fiebig, M., Fjaraa, A. M., Asmi, E., Sellegri, K., Depuy, R., Venzac, H., Villani, P., Laj, P.,  
8 Aalto, P., Ogren, J. A., Swietlicki, E., Williams, P., Roldin, P., Quincey, P., Hüglin, C., Fierz-  
9 Schmidhauser, R., Gysel, M., Weingartner, E., Riccobono, F., Santos, S., Gruning, C., Faloon, K.,  
10 Beddows, D., Harrison, R. M., Monahan, C., Jennings, S. G., O'Dowd, C. D., Marinoni, A., Horn, H. G.,  
11 Keck, L., Jiang, J., Scheckman, J., McMurry, P. H., Deng, Z., Zhao, C. S., Moerman, M., Henzing, B., de  
12 Leeuw, G., Loschau, G., and Bastian, S.: Mobility particle size spectrometers: harmonization of technical  
13 standards and data structure to facilitate high quality long-term observations of atmospheric particle  
14 number size distributions, *Atmos. Meas. Tech.*, 5, 657-685, DOI 10.5194/amt-5-657-2012, 2012.
- 15 Wu, Z. J., Nowak, A., Poulain, L., Herrmann, H., and Wiedensohler, A.: Hygroscopic behavior of  
16 atmospherically relevant water-soluble carboxylic salts and their influence on the water uptake of  
17 ammonium sulfate, *Atmos. Chem. Phys.*, 11, 12617-12626, 10.5194/acp-11-12617-2011, 2011.
- 18 Wu, Z. J., Poulain, L., Henning, S., Dieckmann, K., Birmili, W., Merkel, M., van Pinxteren, D., Spindler,  
19 G., Mueller, K., Stratmann, F., Herrmann, H., and Wiedensohler, A.: Relating particle hygroscopicity and  
20 CCN activity to chemical composition during the HCCT-2010 field campaign, *Atmospheric Chemistry  
21 and Physics*, 13, 7983-7996, 10.5194/acp-13-7983-2013, 2013.
- 22 Yue, D. L., Hu, M., Zhang, R. Y., Wang, Z. B., Zheng, J., Wu, Z. J., Wiedensohler, A., He, L. Y., Huang,  
23 X. F., and Zhu, T.: The roles of sulfuric acid in new particle formation and growth in the mega-city of  
24 Beijing, *Atmos. Chem. Phys.*, 10, 4953-4960, DOI 10.5194/acp-10-4953-2010, 2010.
- 25 Yue, D. L., Hu, M., Zhang, R. Y., Wu, Z. J., Su, H., Wang, Z. B., Peng, J. F., He, L. Y., Huang, X. F.,  
26 Gong, Y. G., and Wiedensohler, A.: Potential contribution of new particle formation to cloud  
27 condensation nuclei in Beijing, *Atmospheric Environment*, 45, 6070-6077,  
28 <http://dx.doi.org/10.1016/j.atmosenv.2011.07.037>, 2011.
- 29 Zdanovskii, B.: Novyi Metod Rascheta Rastvorimostei Elektrolitov v Mnogokomponentnykh Sistema, ,  
30 *Zh. Fiz. Khim+*, 22, 1478-1485, 1486-1495, 1948.
- 31 Zhang, Q., Stanier, C. O., Canagaratna, M. R., Jayne, J. T., Worsnop, D. R., Pandis, S. N., and Jimenez, J.  
32 L.: Insights into the Chemistry of New Particle Formation and Growth Events in Pittsburgh Based on  
33 Aerosol Mass Spectrometry, *Environmental Science & Technology*, 38, 4797-4809, 10.1021/es035417u,  
34 2004a.
- 35 Zhang, R., Suh, I., Zhao, J., Zhang, D., Fortner, E. C., Tie, X., Molina, L. T., and Molina, M. J.:  
36 Atmospheric New Particle Formation Enhanced by Organic Acids, *Science*, 304, 1487-1490,  
37 10.1126/science.1095139, 2004b.



1 Zhu, Y., Hinds, W. C., Kim, S., and Sioutas, C.: Concentration and Size Distribution of Ultrafine  
2 Particles Near a Major Highway, Journal of the Air & Waste Management Association, 52, 1032-1042,  
3 10.1080/10473289.2002.10470842, 2002.

4

5

6

7

8

9

10

11

12

13

14

15

16

17

18

19

20

21

22

23

24

25

1 **Tables and figures**

2

3 Table 1: The summary of instruments and parameters used in this study.

Instrument	Parameter
TDMPS	Particle number size distribution
H-TDMA	Particle hygroscopicity
HR-ToF-AMS	Size-resolved chemical composition
Monitor – APSA 360 Horiba Europe	SO <sub>2</sub> concentration
Kipp & Zonen CM6 Pyranometer	Global solar irradiance

4

5

6 Table 2: Gravimetric densities  $\rho$  and hygroscopicity parameters  $\kappa$ .

Species	NH <sub>4</sub> NO <sub>3</sub>	H <sub>2</sub> SO <sub>4</sub>	NH <sub>4</sub> HSO <sub>4</sub>	(NH <sub>4</sub> ) <sub>2</sub> SO <sub>4</sub>	Organic matter
$\rho$ [kg/m <sup>3</sup> ]	1720	1830	1780	1769	1400
$\kappa$	0.67	0.92	0.61	0.61	0.1

7

8

9 Table 3: The water soluble fraction of newly formed particles and the ratios of H<sub>2</sub>SO<sub>4</sub>  
10 condensational growth to the observed particle growth

Dp	35 nm		50 nm		75 nm	
Date	$\epsilon$	$F_{GR_{H_2SO_4}}$ *	$\epsilon$	$F_{GR_{H_2SO_4}}$	$\epsilon$	$F_{GR_{H_2SO_4}}$
05-06-2008	--		24%	23%	20%	15%
06-06-2008	25%	23%	14%	17%	10%	11%
07-06-2008	34%	30%	23%	20%	17%	13%

11 \*  $F_{GR_{H_2SO_4}} = GR_{H_2SO_4} / GR_{obs}$ : The ratio of H<sub>2</sub>SO<sub>4</sub> condensational growth to the observed particle  
12 growth. Here, GR<sub>obs</sub>s for 35, 50, and 75 nm were calculated over the time period during which Dm of  
13 log-normal ultrafine particle mode grew to 35, 50, and 75 nm, respectively, as indicated by the white  
14 circles in the Fig.1 (a).

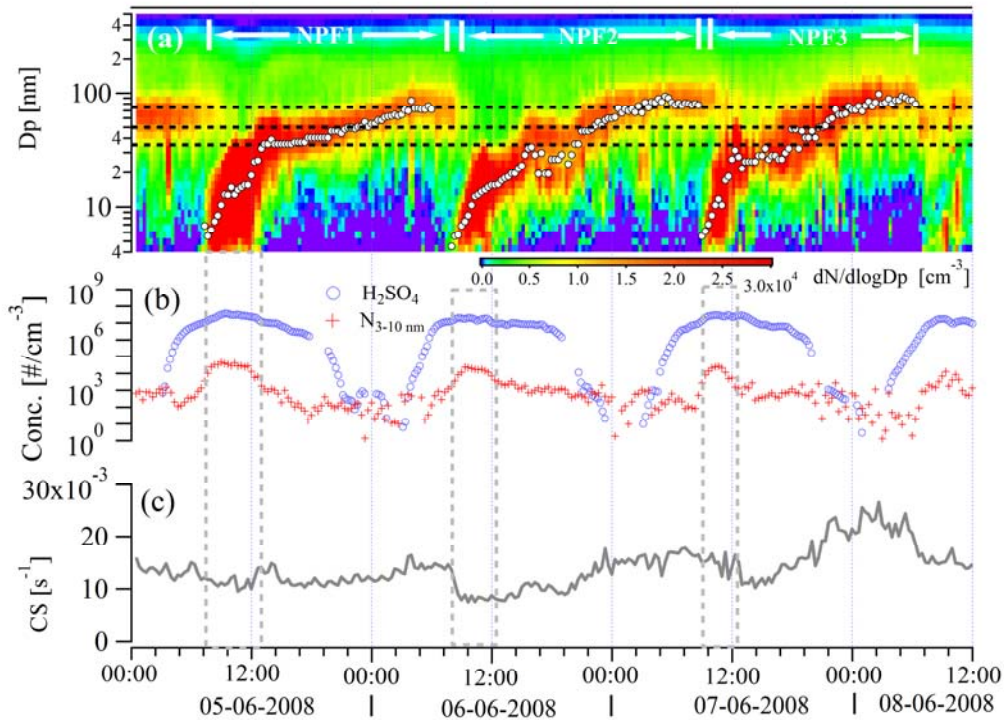
15

16

17

18

1  
2



3

4 Fig. 1: Particle number size distribution (a), 3-10 nm particle number concentration and  $\text{H}_2\text{SO}_4$   
5 concentration (b), condensation sink (CS) (c) during the NPF events. The starting and ending  
6 time of the events were marked in the upper place of panel (a) by NPF1, NPF2, and NPF3. The  
7 while circles in the panel (a) are the  $D_m$  of new particles modes. The grey dashed lines indicated  
8 the time period of particle formation. The black dashed lines in panel (a) indicate the particle  
9 sizes of 35, 50, and 75 nm. In the panel (b), the particle number concentration and  $\text{H}_2\text{SO}_4$   
10 concentration share the same y axis and the unit.

11

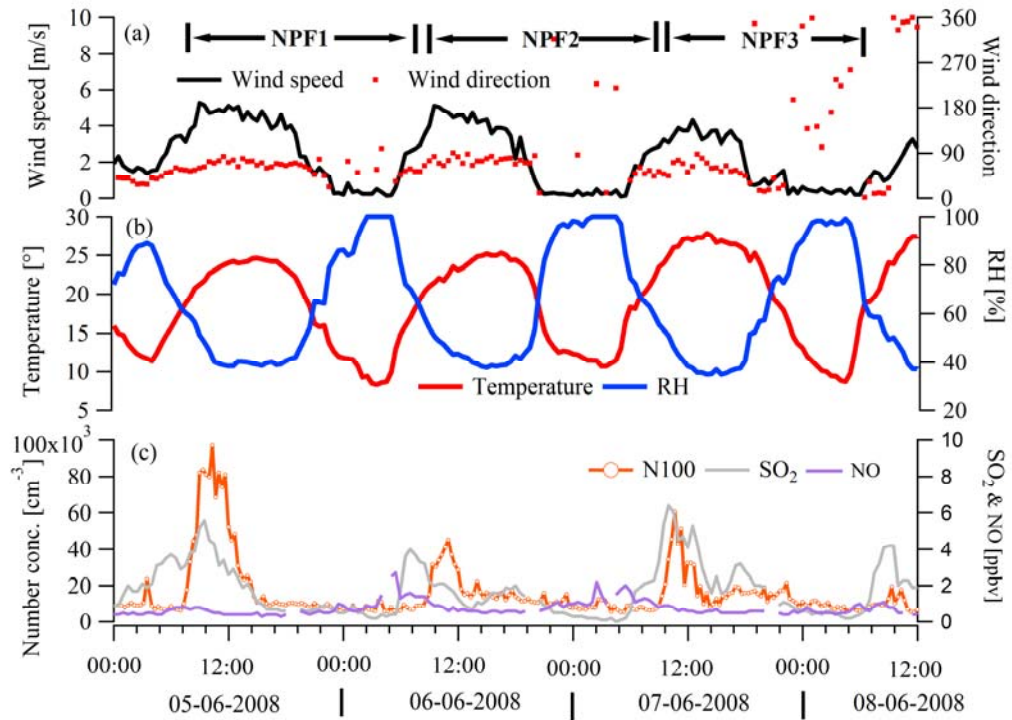
12

13

14

1

2



3

4 Fig. 2: The time series of wind speed and wind direction (a), ambient temperature and RH (b),  
5 and SO<sub>2</sub> & NO concentrations and number concentrations of particles in diameters of 3-100 nm  
6 (b). The starting and ending time of the events were marked in the upper place of panel (a) by  
7 NPF1, NPF2, and NPF3.

8

9

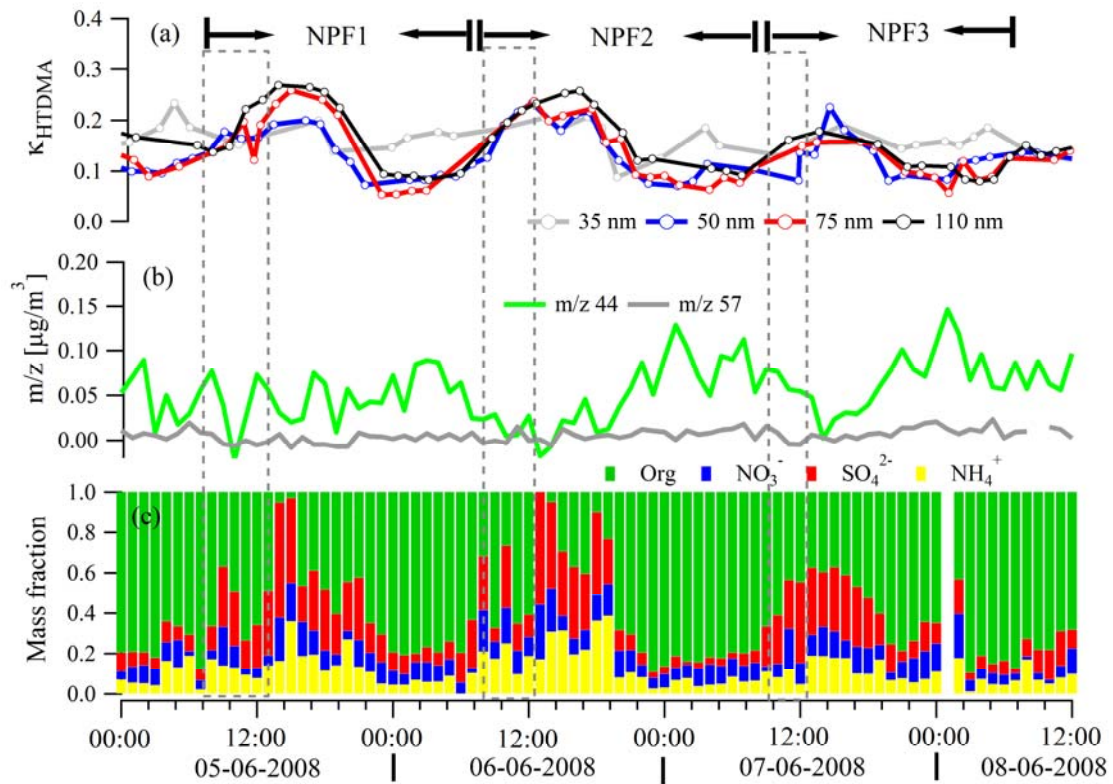
10

11

12

13

1



2

3 Fig.3: Size-resolved particle hygroscopicity (a),  $m/z$  44 and 57 mass concentrations in 30-100 nm  
4 particles (b), and mass fraction of organic, sulfate, nitrate, and ammonium in 30-100 nm particles (c). The  
5 grey dashed lines indicated the time period of particle formation.

6

7

8

9

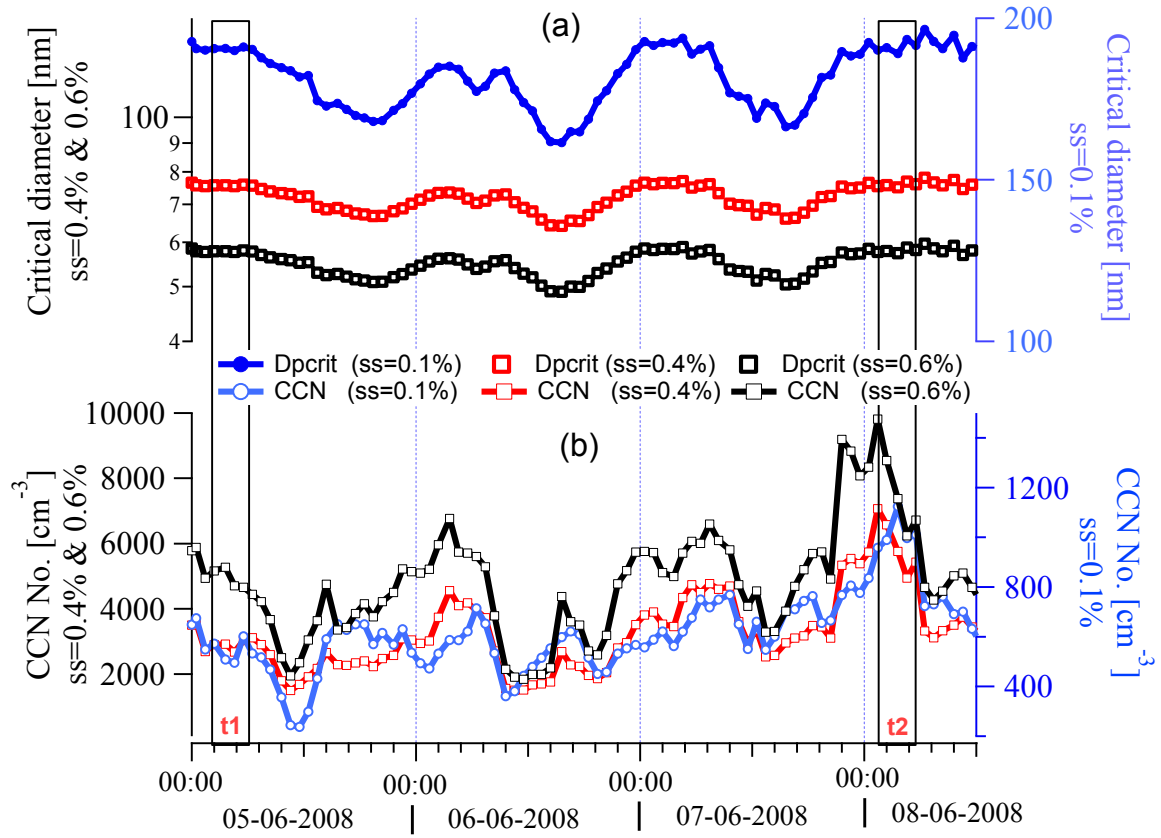
10

11

12

1

2



3

4

Fig. 4: Critical diameter (Dpcrit) and CCN number concentration during NPF events.

5